RECEIVED

SEP 2 4 1964

Reactor Design

WANL-TMI-1257

From Engineering Mechanics

Date September 22, 1964

Subject Discussion of Data - EML-1 Reactor Ass'y. Axial Vibr. Test - Nozzle Excitation

WESTINGHOUSE ASTRONUCLEAR LABORATORY

Mr. W. J. Rowan, Manager
Engineering Mechanics

cc:

Arnold, W. H.	Henning, F. W.	Spurrier, F. R.
Bifano, N. J.	Manjoine, M. J.	Tauch, F. G.
Bournia, A.	McCreary, H. S.	Thompson, D. C.
Brussalis, W. G.	Miller, D. F.	Tully, J. P.
Cernie, S.	Price, J. L.	Warner, P. C.
DeZubay, E. A.	Retallick, F. D.	Watjen, E. A.
Esselman, W. H.	Rieke, K. L.	Wisniewski, E. J.
Faught, H. F.	Roman, W. G.	Library
Gallagher, J. G.	Selz, A.	File

This letter discusses the data recorded during the nozzle flange excitation of the ND-20102 reactor. The test environment and Series 35, 36 and 37 set of transducers are described in EE-3709 and TMI-1258. Typical samples of data are presented in TMI-1259 and are referred to in this memorandum.

INFORMATION CATEGORY
Unclassified
D. F. Miller 9-23-64

lec

DISCLAIMER

SUMMARY:

Frequencies of special interest are 62, 150, 400, 500, 1200 and 1700 cps. Pressure vessel, outer reflector and core support plate exhibit acceleration magnification at 62 cps. At 150 cps, the core motions are amplified. At 400 cps, the pressure vessel, outer reflector and core are moving, exhibiting relative acceleration magnifications. The core support plate shows a resonance at 500 cps. Other resonances occurring at 1200 and 1700 cps require further study.

TEST RESULTS:

The maximum transducer outputs are listed in Tables I and II. Table III summarizes the acceleration characteristics of the mass-spring system. This system had been previously studied on the computer.

The system impedance plots are shown in the Group C curves of TMI-1259. Major component response plots are shown in the Group D curves. The X-Y response plots shown are for a 1 G sweep. Control of the input acceleration was at the nozzle flange. In the frequency range from 50 - 90 cps, the input was manually held below 1 G because of excessive force requirements.

A high system impedance exists at 62 cps. Pressure vessel magnifications occur at 62 and at 400 cps. Outer reflector magnifications occur at 62 and at 400 cps. Core magnifications as measured on a support block accelerometer, occur at 150 and 400 cps. Support plate magnifications occur at 62,400 and 500 cps.

At 62 cps the pressure vessel and outer reflector are moving together and are magnified over the input by a factor of 2-1/2 to 1. This anti-resonance point appears to be a result of the simulated pressure vessel nozzle flexibility. A probe test of the pressure vessel at this frequency indicates that it acts as a single mass.

At 400 cps the pressure vessel, outer reflector and core accelerations are magnified. The dome end support ring could be the cause of this magnification as a phase shift occurs at this frequency between the pressure vessel and outer reflector.

TABLE I
TRANSDUCER DATA SUMMARY SHEET

Transducer Code	Description	Measurement Made	Maximum Value Monitored					
			Frequency (CPS)	Input (G)	Value μ "/"	Frequency (CPS)	Input (G)	Value μ "/"
S62	2H5 Fuel Element	Strain	All	All	<25	-	-	-
S78	3E3 Fuel Element	"	"	"	<45	-	-	-
S153	1E4 Tie Rod - T1	"	400	1.25	15	99	0.57	14.3
S154	1E4 Tie Rod - T2	"	500	.59	13.2	400	1.28	4.5
S157	2H5 Tie Rod - T1	"	104	1.02	150	49	0.9	95
S158	2H5 Tie Rod - T2	"	60	0.65	180	24	0.7	100
S452	Tie Bolt	"	104	1.28	50	All	0.3 & 0.6	<20
S500	Core Support Ring	"	74	0.93	45	62	0.6	38
S502	Core Support Ring	"	79	0.86	60	121	0.85	45
S503	Core Support Ring	"	All	All	<30	-	-	-
S504	Core Support Ring	"	74	1.09	45	62	0.6	35
S506	Core Support Ring	"	74	1.09	25	All	0.3 & 0.6	<15
S550	Dome End Support Ring	"	89	1.02	35	All	0.3 & 0.6	<20
S552	Dome End Support Ring	"	89	1.02	60	65	0.7	50
S570	Bolt	"	74	1.09	40	63	0.6	40
S573	Bolt	"	All	All	<10	-	-	-

TABLE II
TRANSDUCER DATA SUMMARY SHEET

Transducer Code	Description	Measurement Made	Maximum Value Monitored					
			Frequency (CPS)	Input (G)	Value (G)	Frequency (CPS)	Input (G)	Value (G)
A200	Pressure Vessel (Dome)	Radial Acceleration	179	1.04	27	178	0.7	19.2
A201	Pressure Vessel (Mid)	" "	179	1.04	18	178	0.7	17.2
A202	Pressure Vessel (Nozzle)	" "	267	1.0	>11	178	0.7	>11
A212	Pressure Vessel (Nozzle)	Axial Acceleration	79	0.85	1.72	60	0.9	1.25
A230	Outer Reflector	" "	72	1.04	2.5	64 & 107	0.85	1.7
A231	Outer Reflector	" "	128	1.35	1.6	108	0.55	1.4
A232	Outer Reflector	" "	122	1.25	1.8	110	0.57	1.4
A240	Control Drum	Radial Acceleration	101	0.56	4.5	81	0.42	2.73
A242	Control Drum	" "	79	0.55	13.0	75	0.26	3.8
A250	Bearing Housing	Axial Acceleration	<165	1.0	> 2.5	-	-	-
A252	Bearing Housing	" "	<145	1.0	>5.0	-	-	-
A254	Control Drum Shaft	" "	89	0.46	23.4	96	0.43	7.5
A255	Control Drum Shaft	Radial Acceleration	87	0.55	123	122	1.28	25.0
A256	Control Drum Shaft	" "	89	0.46	11.4	119	1.21	6.0
A355	6B1 Support Block	Axial Acceleration	142	0.94	1.9	69	0.7	1.0
A356	6H6 Support Block	" "	142	0.94	1.75	-	-	-
A362	Support Plate Periphery	" "	69 & 107	0.85	2.5	76	1.09	2.5
A371	Support Plate Center	" "	72	0.93	3.2	69	0.7	2.3

TABLE III
SUMMARY CHART

Ref: Series 35, Test 1, Run 3; Series 36, Test 1, Run 3

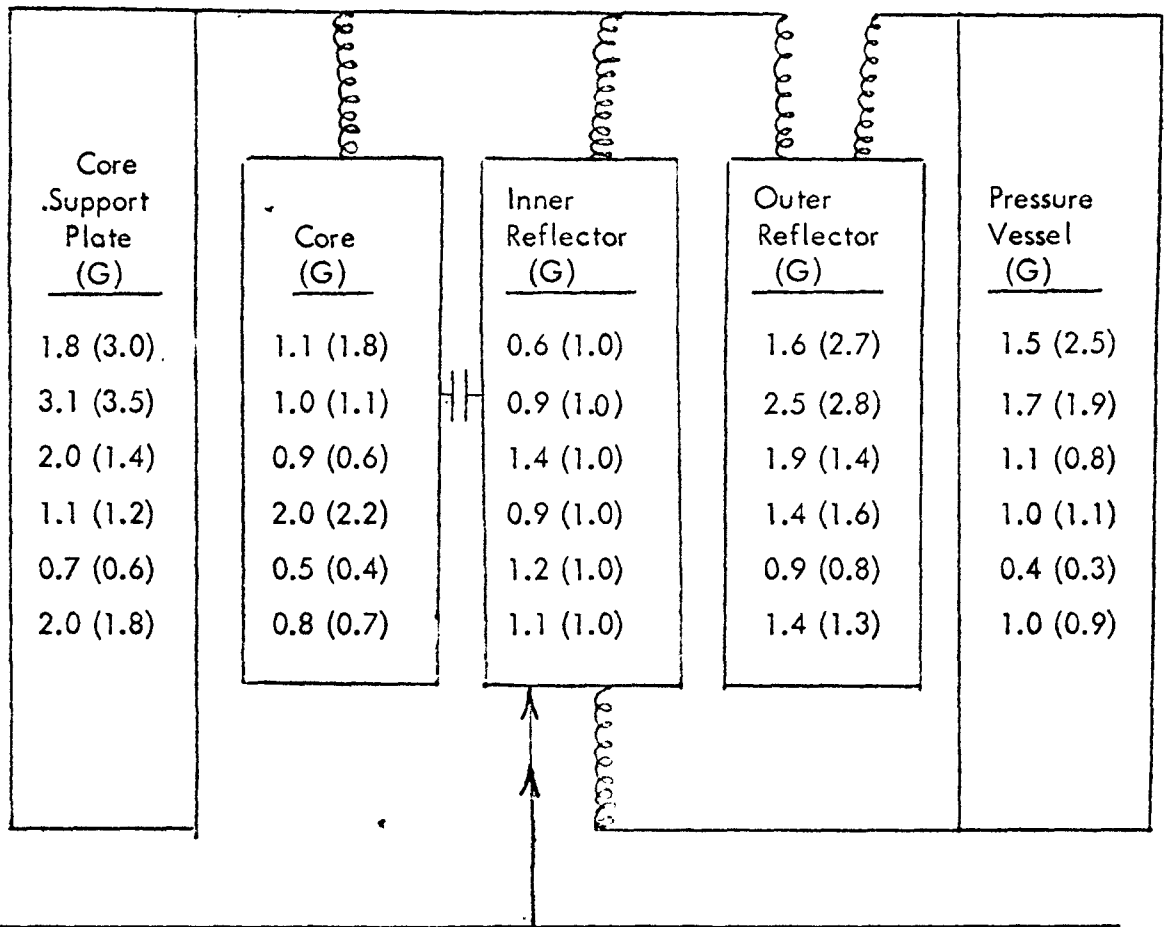

Frequency (CPS)	Core Support Plate (G)	Core (G)	Inner Reflector (G)	Outer Reflector (G)	Pressure Vessel (G)
62	1.8 (3.0)	1.1 (1.8)	0.6 (1.0)	1.6 (2.7)	1.5 (2.5)
72	3.1 (3.5)	1.0 (1.1)	0.9 (1.0)	2.5 (2.8)	1.7 (1.9)
120	2.0 (1.4)	0.9 (0.6)	1.4 (1.0)	1.9 (1.4)	1.1 (0.8)
145	1.1 (1.2)	2.0 (2.2)	0.9 (1.0)	1.4 (1.6)	1.0 (1.1)
340	0.7 (0.6)	0.5 (0.4)	1.2 (1.0)	0.9 (0.8)	0.4 (0.3)
370	2.0 (1.8)	0.8 (0.7)	1.1 (1.0)	1.4 (1.3)	1.0 (0.9)

Frequency (CPS)	Acceleration (G)	Thruster Force (lb)	Input Impedance (lb-sec/inch)
62	0.6	9835	37,000
68	0.9	10330	28,300
72	0.9	10760	18,800
120	1.4	3275	5,250
145	0.9	3513	7,700
340	1.2	524	2,010
360	1.2	457	2,750
370	1.1	800	4,950

NOTE: Values in parenthesis normalized to 1.0 G input.

At 150 cps, core motion exhibits a phase shift to that of the outer reflector, and core support plate indicating that the tie rod stiffness may be acting on the system. An amplification of tie rod strain is present at this frequency.

The core support plate magnification at 500 cps appears to be caused by the core support ring stiffness.

Accelerometers mounted at both ends of the drive cone indicate that it remained rigid to 400 cps. The impedance plots are, therefore, numerically meaningful to this frequency.

Magnifications also occur on many transducers at frequencies of 400, 1200 and 1700 cps. These higher frequency responses could be significant and are presently being investigated.

The strain in the reactor components were relatively low during Series 35 and 36 as seen in Table I. The fuel element strains were less than the channel noise level. The tie rod strain occurred, as expected, at the frequency where the differential acceleration between core and core support plate is the greatest.

The highest core support ring strain occurred at frequencies where the core support plate has its largest accelerations.

Dome end support ring strains were monitored at frequencies where the largest acceleration differential between pressure vessel and outer reflector occur.

The bolts in the core support ring show a maximum at the frequency where the core support plate exhibits its maximum acceleration.

The test data compares favorably with the analog results as seen from Group A curves in TMI-1259.

The lumped mass model used for the analog study is shown in Figure 1.

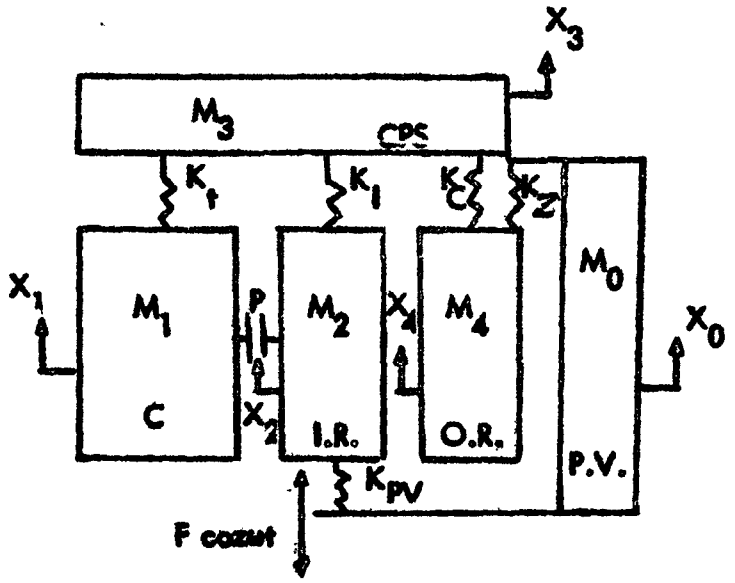

Figure 1

The equations of motions are:

$$M_2\ddot{X}_2 + K_{PV}(X_2 - X_0) + K_1(X_2 - X_3) \pm P = \quad = F_{coolant}$$

$$M_0\ddot{X}_0 + K_Z(X_0 - X_4) + K_{PV}(X_0 - X_2) \quad = 0$$

$$M_1\ddot{X}_1 + K_T(X_1 - X_3) \mp P \quad = 0$$

$$M_3\ddot{X}_3 + K_T(X_3 - X_1) + K_C(X_3 - X_4) + K_1(X_3 - X_2) = 0$$

$$M_4\ddot{X}_4 + K_Z(X_4 - X_0) + K_C(X_4 - X_3) \quad = 0$$

where

M_0	- 2000 lb	Pressure Vessel
M_1	- 3000 lb	Core
M_2	- 725 lb	Inner Reflector
M_3	- 370 lb	Support Plate
M_4	- 2490 lb	Outer Reflector

K_{PV}	$- 1.7 \times 10^6$ lb/in.	Pressure Vessel
K_Z	$- 6.5 \times 10^6$ lb/in.	Dome End Support Ring
K_C	$- 16 \times 10^6$ lb/in.	Core Support Cone
K_T	$- 1.4 \times 10^6$ lb/in.	Tie Rods
P	- 4000 lb	Friction
K_I	- 18,000 lb/in.	Inner Reflector Preload

The support cone and dome end support ring stiffness was obtained from C-2 static test data. As a comparison, the calculated stiffness of these two components, ignoring local bending effects, are 32×10^6 lb/in. and 13×10^6 lb/in. respectively. The tie rod stiffness value was calculated analytically. The stiffness value used for the pressure vessel represents local deflection at the nozzle flange. This value was obtained in a lab test where the flange was loaded to 10,000 lb using a hydraulic jack. The barrel stiffness, neglecting local flange deflection, is 14.8×10^6 lb/in.

Static tests on an Aerojet pressure vessel indicate a total stiffness of 16.2×10^6 lb/in. between the dome end and nozzle flange. (Value obtained in a telephone conversation with Edward Snyder of Aerojet.) This high stiffness value indicates that no local deflection is occurring at the Aerojet nozzle flange.

The lab test which determined that local deflection does occur on the simulated pressure vessel was of necessity performed quickly at less than ideal conditions. In order to completely analyze EML-1 test data and relate it to A-2 conditions, the simulated pressure vessel stiffness will be verified at the first disassembly.

The feasibility of analyzing the reactor with a lumped mass model shows promise. From all indications a refinement of the analog input can be made to duplicate the motions of the primary reactor components. The following component characteristics are singled out so that a comparison can be made with field data.

Drive Force

A peak value comparison is shown in Curve A-1*. There appears to be a frequency shift of approximately 15 cps. The wave forms for the analog and test

* Presented in TMI-1259.

are seen to be sinusoidal from Figures B1* through B3* and in Figures D4*, D6*, and D8*. Some noise is present in D6* and D8*.

Core

The greatest deviation between the test and analog results occur in Curve A2*. The core motions were measured by an accelerometer mounted to a support block located on the 6B1 and 6H6 clusters. From the accelerometer outputs monitored, the core moves as a lumped mass at frequencies less than 220 cps. The acceleration of the support block at 6B1 is approximately twice that at 6H6 between the frequencies at 220 to 400 cps, indicating the core no longer remains as a rigid mass. For frequencies greater than 400 cps, the core motion is isolated from the driving force.

The waveshape comparison between test and analog reveal the motion to be non-sinusoidal at frequencies less than 95 cps as seen in B7*, B8*, B9* and D10*.

Core Support Plate

Curve A-3* shows a similar 15 cps shift in frequency to that noted in the drive force data comparison. The core support plate Curves D11* shows a maximum acceleration level at 72 cps. Strain in the core support ring is a maximum at approximately the same frequency as seen from Table I. Support plate amplifications greater than 1 occur at 370 cps, 510 cps and between 17 to 160 cps. Similarly for the analog model, this amplification takes place between 20 cps and 110 cps.

Outer Reflector

The outer reflector exhibits the same 15 cps frequency shift as for the force and core support plate. The core support plate and outer reflector show similar amplification build-ups for the test and analog data as seen in A3* and A4*. For the analog data, the core support plate indicates a slightly higher damping constant. During the laboratory test, the damping constant is smaller for the core support plate than for the outer reflector. In general, the core support plate and outer reflector show the same motion characteristic as seen in D11 and D13*.

* Presented in TMI-1259.

Pressure Vessel

Curve A5* shows that the pressure vessel damping is higher than was assumed for the analog model. Amplification occurs at 370 cps and between 160 and 25 cps.

Group A* curves, as summarized in Table III, give a good insight into the motion characteristics of the major reactor components. High impedance occurs at approximately 62 cps when all components are moving at maximum acceleration levels as seen in Group A curves. This can be considered as false antiresonant point due to the fact that the spring constant K_{PV} in Figure 1 is simulated. As previously noted, the simulated pressure vessel is only 9.5% as stiff as the Aerojet pressure vessel.

Any questions regarding the tests should be directed to the writers.

---

* Presented in TMI-1259.

R. D. Burack
Reactor Assembly & Dynamics Experiments

N. J. Ettenson
Reactor Assembly & Dynamics Experiments

Approved:

D. F. Miller, Supervisor
Reactor Assembly & Dynamics Experiments

lec